Published online 13 November 2007

Nucleic Acids Research, 2008, Vol. 36, No. 1 ***121–132***
doi:10.1093/nar/gkm913

Distinct HDACs regulate the transcriptional response of human cyclin-dependent kinase inhibitor genes to trichostatin A and 1α,25-dihydroxyvitamin D_3

Marjo Malinen[1], Anna Saramäki[1], Antti Ropponen[2], Tatjana Degenhardt[1], Sami Väisänen[1] and Carsten Carlberg[1,3,*]

[1]Departments of Biochemistry, [2]Clinical Microbiology, University of Kuopio, FIN-70211 Kuopio, Finland and [3]Life Sciences Research Unit, University of Luxembourg, L-1511 Luxembourg, Luxembourg

Received June 13, 2007; Revised September 4, 2007; Accepted October 8, 2007

ABSTRACT

The anti-proliferative effects of histone deacetylase (HDAC) inhibitors and 1α,25-dihydroxyvitamin D_3 [1α,25$(OH)_2D_3$] converge via the interaction of un-liganded vitamin D receptor (VDR) with co-repressors recruiting multiprotein complexes containing HDACs and via the induction of cyclin-dependent kinase inhibitor (*CDKI*) genes of the INK4 and Cip/Kip family. We investigated the effects of the HDAC inhibitor Trichostatin A (TSA) and 1α,25$(OH)_2D_3$ on the proliferation and *CDKI* gene expression in malignant and non-malignant mammary epithelial cell lines. TSA induced the INK4-family genes *p18* and *p19*, whereas the Cip/Kip family gene *p21* was stimulated by 1α,25$(OH)_2D_3$. Chromatin immunoprecipitation and RNA inhibition assays showed that the co-repressor NCoR1 and some HDAC family members complexed un-liganded VDR and repressed the basal level of *CDKI* genes, but their role in regulating *CDKI* gene expression by TSA and 1α,25$(OH)_2D_3$ were contrary. HDAC3 and HDAC7 attenuated 1α,25$(OH)_2D_3$-dependent induction of the *p21* gene, for which NCoR1 is essential. In contrast, TSA-mediated induction of the *p18* gene was dependent on HDAC3 and HDAC4, but was opposed by NCoR1 and un-liganded VDR. This suggests that the attenuation of the response to TSA by NCoR1 or that to 1α,25$(OH)_2D_3$ by HDACs can be overcome by their combined application achieving maximal induction of anti-proliferative target genes.

INTRODUCTION

The classical role of histone deacetylases (HDACs) is to reduce transcription by the removal of acetyl groups from histones, a process that makes the DNA bind to the histones more tightly (1). The mammalian HDAC gene family is categorized into three classes (2). Class I includes HDACs 1, 2, 3 and 8 and class II HDACs 4, 5, 6, 7, 9 and 10. HDAC11 shares characters of both classes I and II. Class I HDACs are ubiquitously expressed and have general roles in homeostasis, signal transduction, cell cycle control and cancer development (3). HDAC3 is tightly linked to gene regulation by nuclear receptors through its functional connection to co-repressors. This HDAC also has a transcription-independent role in mitosis as well as functions in cell cycle progression and stem cell renewal (3,4). Class II HDACs, namely HDACs 4, 5, 7 and 9, are expressed tissue-specifically and shuttle between the nucleus and the cytoplasm in a stimulus-dependent manner (5). HDAC7 suppresses apoptosis in thymocytes via the orphan nuclear receptor Nurr77 (6). HDAC6 is the only HDAC identified to deactylate tubulin and this capacity is required for its function in aggrosomes, through which it affects the disposal of misfolded proteins (7). All class I and II HDACs are sensitive to the inhibitor Trichostatin A (TSA) (8). In contrast, the members of the third HDAC class, SIRT1 to 7, are TSA insensitive. Although the roles of individual HDACs in cancer are unsolved, HDAC inhibitors are of interest to the medical community because they have been shown in numerous experiments to reduce cancer cell growth and enhance cell differentiation. They are thought to exert this effect by effecting changes in the gene expression of the cyclin-dependent kinase inhibitor (*CDKI*) genes *p18*, *p19* and *p21*

*To whom correspondence should be addressed. Tel: +352 4666446267; Fax: +352 4666446435; Email: carsten.carlberg@uni.lu

The authors wish it to be known that, in their opinion, the first two authors should be regarded as joint First Authors.

as well as *cyclin* genes (9–12). HDAC inhibitors induce the accumulation of acetylated histones on the *p21* promoter, whereas on the *CDKI* gene *p27* no change was observed (10,13).

The cell cycle transition between the first gap phase (G_1) to DNA synthesis phase (S) is co-operatively regulated by several classes of cyclin-dependent kinases (CDKs). CDKs hyperphosphorylate the retinoblastoma protein, which then releases E2F family transcription factors needed for the entry into the S phase. CDKs activities are turned off by CDKI proteins. CDKIs are a group of low molecular weight proteins that associate with cyclin–CDK complexes or CDKs alone and inhibit their activity. Most tumors carry mutations or epigenetic malfunctions in regulators of CDKs, but not in CDKs themselves. In cancer treatment this common misregulation of CDK regulators has not yet been successfully targeted in clinical trails (14). The INK4 subfamily of CDKIs includes closely related genes *p15* (*INK4B* or *CDKN2B*), *p16* (*INK4A* or *CDKN2A*), *p14* (*ARF*, also transcribed from *CDKN2A*), *p18* (*INK4C* or *CDKN2C*) and *p19* (*INK4D* or *CDKN2D*). The protein products of this gene family specifically bind and inhibit CDK4 and CDK6, which prevent cyclin D-dependent phosphorylation of the retinoblastoma protein (15,16). The CDKIs *p21* (*WAF1*/*Cip1* or *CDKN1A*), *p27* (*Kip1* or *CDKN1B*) and *p57* (*Kip2* or *CDKN1C*) belong to the CIP/KIP family. They selectively inhibit the association of cyclin A, D and E with CDK complexes and thus control the G_1 to S phase transition in the mammalian cell cycle. We recently demonstrated three functional vitamin D receptor (VDR)-associated regions on the *p21* promoter *in vivo* (17). Vitamin D response elements are positioned at −2.3 kB, −4.5 kB and −6.9 kB from the transcription start site (TSS) of the *p21* gene with p53 binding co-localized in two of these regions. Concomitantly, *p21* has been shown to be one of the key genes for anti-proliferative action of 1α,25-dihydroxyvitamin D_3 [1α,25$(OH)_2D_3$] (18). In contrast, p27 is a short-lived protein and its activity is regulated almost exclusively post-translationally by the ubiquitin–proteosome protein degradation system. Decreased p27 protein levels are common in many tumor types (19).

VDR is a member of the nuclear receptor superfamily and acts as a transcription factor by binding to specific response elements in its target genes. In the absence of ligand, VDR associates via co-repressor proteins, such as NCoR1 and SMRT/NCoR2, with HDACs (20). This complex represses gene transcription by stabilizing DNA–histone contact and closing chromatin structure. The natural VDR ligand 1α,25$(OH)_2D_3$ has an essential role in calcium homeostasis and skeletal integrity (21), but also an important role in the regulation of cell growth and differentiation (22). The ligand binds the VDR with high affinity, changes the conformation of its ligand-binding domain, so that it is more favorable for the binding of co-activator proteins (23) after the co-repressor/HDAC complex has dissociated.

By combining different therapeutic compounds, that target transcription of genes, it might be possible to sensitize cancer cells to particular chemotherapies. Therefore, in this study we investigated the effects of TSA and 1α,25$(OH)_2D_3$ on the proliferation and *CDKI* gene expression in malignant and non-malignant mammary epithelial cell lines. TSA induced the genes *p18* and *p19*, whereas the *p21* gene was stimulated by 1α,25$(OH)_2D_3$. Chromatin immuno-precipitation (ChIP) and RNA inhibition (RNAi) assays showed that NCoR1 and certain HDAC family members complexed un-liganded VDR and repressed the basal level of *CDKI* genes, but their role in regulating *CDKI* gene expression by 1α,25$(OH)_2D_3$ and TSA were contrary. HDAC3 and HDAC7 attenuated 1α,25$(OH)_2D_3$-dependent induction of *p21*, for which NCoR1 is essential. TSA-mediated induction was dependent on HDAC3 and HDAC4, but was opposed by NCoR1 and un-liganded VDR. This suggests that the attenuation of the response to 1α,25$(OH)_2D_3$ by HDACs or the response to TSA by NCoR1 can be overcome by their combined application achieving maximal induction of anti-proliferative target genes.

MATERIALS AND METHODS

Cell culture

MCF-12A (spontaneously immortalized mammary epithelial) cells were cultured in a mixture of DMEM and Ham's F12 medium (1:1) with 20 ng/ml of epidermal growth factor, 100 ng/ml of cholera toxin, 10 μg/ml insulin, 500 ng/ml hydrocortisone and 5% horse serum. MCF-7 (mammary epithelial adenocarcinoma) cells were grown in α-MEM supplemented with 7% fetal bovine serum (FBS). MDA-MB453 (mammary epithelial metastatic carcinoma) cells were grown in α-MEM supplemented with 10% FBS. All cell lines were grown in a humidified 95% air/5% CO_2 incubator. Before mRNA extraction or ChIP assay, MCF-7 and MDA-MB453 cells were grown overnight in phenol red free DMEM with 5% charcoal-stripped FBS and MCF-12A in above-mentioned culture medium but with 5% charcoal-stripped FBS instead of horse serum. The cells were treated at a density of 50–60% confluency for indicated time periods with 15 nM TSA (Sigma Aldrich, diluted in EtOH) and/or 10 nM 1α,25$(OH)_2D_3$ (kindly provided by Dr Lise Binderup, LEO Pharma, Ballerup, Denmark, diluted in EtOH) or EtOH (0.1%).

Proliferation, cell cycle and cell growth analysis

Cell proliferation levels were studied by 5-bromo-2-deoxyuridine (BrdU) incorporation. For measuring relative proliferation levels the Cell Proliferation ELISA kit (Roche) was used as instructed by the manufacturer. Cell cycle analysis was performed by propidium iodide DNA staining. Fixation and staining of the cells were performed according to standard protocols. Briefly, after 48 h incubation with ligands or vehicle cells were harvested by trypsinization and fixed with ice-cold 70% EtOH. After overnight incubation at 4°C, cells were centrifuged and incubated in 1 ml RNAase A solution (150 μg/ml RNAase A in phosphate-buffered saline (PBS, 140 mM NaCl, 2.7 mM KCl, 1.5 mM KH_2PO_4, 8.1 mM $Na_2HPO_4.2H_2O$)) for 1 h at 50°C. Propidium iodide in PBS was added to the final concentration of 8 μg/ml and

incubation was continued for 2 h at 37°C. To obtain the portion of the cells in the different phases of the cell cycle, DNA content of cells was analyzed using a FACSCanto II flow cytometer with BD FACSDiva Flow Cytometry Software Version 5.0. (Becton Dickinson, Mountain View, CA, USA). For growth analysis, cells were cultured for 5 days in the presence of either vehicle or ligands. Cell numbers were counted using a haemacytometer after the cells had been trypsinized, suspended in PBS supplemented with 5% FBS and stained with the vital dye erythrosine-red.

RNA extraction and real-time quantitative PCR

Total RNA was extracted using the Mini RNA Isolation II kit (Zymo Research, HiSS Diagnostics, Freiburg, Germany) and cDNA synthesis was performed for 1 h at 37°C using 1 μg of total RNA as a template, 100 pmol oligodT15 primer and 40 U reverse transcriptase (Fermentas, Vilnius, Lithuania). Real-time quantitative PCR was performed in an IQ-cycler (BioRad, Hercules, CA, USA) using the dye SybrGreen I (Molecular Probes, Leiden, The Netherlands). Fast Start Taq polymerase (Roche) and 3 mM $MgCl_2$ were used and the PCR cycling conditions were: 40 cycles of 30 s at 95°C, 30 s at 60°C and 30 s at 72°C. The sequences of the gene-specific primer pairs for the human *CDKI* genes *p18*, *p19*, *p21* and *p27* and the control gene *acidic riboprotein P0* (*RPLP0*) are listed in the Table S1. Fold inductions were calculated using the formula $2^{-(\Delta\Delta Ct)}$, where $\Delta\Delta Ct$ is the $\Delta Ct_{(stimulant)} - \Delta Ct_{(EtOH)}$, ΔCt is $Ct_{(CDKI)} - Ct_{(RPLP0)}$ and Ct is the cycle at which the threshold is crossed. Basal expression levels were calculated using the formula $2^{-(\Delta Ct)}$. Quality of the PCR product was monitored using post-PCR melt curve analysis.

ChIP assay. ChIP and re-ChIP were performed as described previously (17), except that formaldehyde cross-linking time was diminished to 5 min and antibodies were used against HDAC1 (sc-6298), HDAC2 (sc-6296), HDAC3 (sc-11417), HDAC4 (sc-11418), HDAC5 (sc-11419), HDAC6 (sc-11420), HDAC7 (sc-11421), VDR (sc-1008) NCoR1 (sc-8994) and RNA polymerase II (Pol II) (sc-899) and normal mouse IgG (sc-2027) as a control (all obtained from Santa Cruz Biotechnologies, Heidelberg, Germany). The anti-acetylated histone 4 (AcH4) and anti-acetylated histone 3, lysine 14 (AcH3-K14) antibodies were obtained from Upstate (Lake Placid, NY, USA).

PCR of chromatin templates

For each of the three VDR-associated regions of the *p21* promoter as well as for the TSS regions of all four *CDKI* genes, specific primer pairs were designed (Table S2), optimized and controlled by running PCR reactions with 25 ng genomic DNA (input) as a template. When running immuno-precipitated DNA (output) as a template, the following PCR profile was used: pre-incubation for 5 min at 95°C, 40 cycles of 30 s at 95°C, 30 s at the primer-specific temperature (Table S2) and 30 s at 72°C and one final incubation for 10 min at 72°C. The PCR products were separated by electrophoresis through 2% agarose gels. Relative acetylation levels were calculated using the formula $2^{-(\Delta Ct)}$ where ΔCt is $Ct_{(output)} - Ct_{(input)}$ and normalized by the amount of chromatin used for preparation of input versus output. Gel images were scanned on a FLA3000 reader (Fuji) using ScienceLab99 software (Fuji).

Chromatin conformation capture (C3) analysis

Chromatin was cross-linked and lysed as for ChIP assays but the sonication was reduced to 2 pulses. After removal of cellular debris by centrifugation, 100 μl of chromatin diluted in 345 μl of ChIP dilution buffer was digested overnight at 37°C with the restriction enzymes MvaI (50 units), Hpy8I (25 units) or SchI (25 units). Digested chromatin was ligated with 50 U T4 DNA ligase (Fermentas) for 2 h at 16°C and then 2 μl of proteinase K (10 mg/ml, Fermentas) was added and the samples were further incubated overnight at 64°C. Finally, the DNA was recovered by phenol–chloroform extraction followed by EtOH precipitation and analyzed by PCR using primers which are listed in Table S3. As positive controls, plasmids covering the *p21* promoter regions −7930 to −6072, −4968 to −3818 or −2620 to −1335 were digested and ligated with plasmid covering the TSS region (−676 to +535).

siRNA inhibition

Cells were grown to 30–40% confluency. MCF-12A cells were transfected using Lipofectamine 2000 (Invitrogen) and MCF-7 and MDA-MB453 cells with Lipofectamine RNAiMAX (Invitrogen) according to the manufacturer's instructions. Double-stranded siRNA oligonucleotides (Eurogentec, 200 pmol of each siRNA, for sequences see Table S4) were transfected for 5 h, then charcoal-stripped FBS was added (5% final concentration) and the transfection was continued for 48 h. Cell treatments, RNA extractions and real-time quantitative PCR were carried out as described above.

RESULTS

Anti-proliferative effects of TSA and 1α,25(OH)$_2$D$_3$ in breast epithelial cells

We have chosen three breast epithelial cell lines MCF-12A, MCF-7 and MDA-MB453 as models for testing anti-proliferative and gene regulatory effects of TSA and 1α,25(OH)$_2$D$_3$. MCF-12A is a spontaneously immortalized cell line, MCF-7 is an estrogen-responsive adenocarcinoma cell line and MDA-MB453 is an estrogen-insensitive metastatic carcinoma cell line. All three cell lines were treated with the relative low doses of 15 nM TSA and 10 nM 1α,25(OH)$_2$D$_3$, alone and in combination, for five days (Figure 1A). Relative proliferation in reference to EtOH-treated cells was then measured by BrdU incorporation. TSA showed a significant anti-proliferative effect only in MCF-7 cells (32% reduction), while 1α,25(OH)$_2$D$_3$ inhibited the growth of MCF-12A, MCF-7 and MDA-MB453 cells by 40, 34 and 42%, respectively. The combinatorial treatment with TSA and

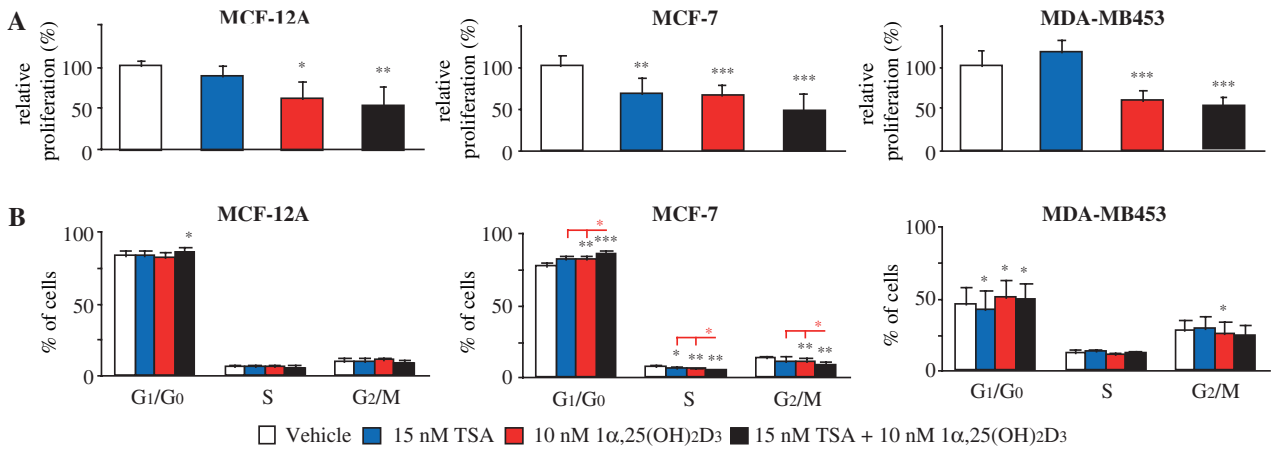

Figure 1. TSA and $1\alpha,25(OH)_2D_3$ inhibit the growth of epithelial breast cancer cells. (**A**) MCF-12A, MCF-7 and MDA-MB453 cells were treated, alone or in combination, with 15 nM TSA, 10 nM $1\alpha,25(OH)_2D_3$ and EtOH every second day for 5 days in total. Cell proliferation levels were measured by BrdU incorporation using a Cell Proliferation ELISA. (**B**) The portion of the cells in the different phases of the cell cycle were determined after 48 h ligand treatment by propidium iodide DNA staining using FACSCanto II flow cytometer analysis. Columns indicate the means of at least three independent cell treatments and the bars represent standard deviations (A and B). A two-tailed Student's *t*-test was performed to determine the significance of the stimulation in reference to vehicle-treated control ($^*P < 0.05$; $^{**}P < 0.01$; $^{***}P < 0.001$). The significance of the co-treatment in comparison to the single stimulations with TSA and $1\alpha,25(OH)_2D_3$ were calculated (red stars).

$1\alpha,25(OH)_2D_3$ resulted in, for all three cell lines, approximately 50% reduced growth compared to EtOH-treated cells. At the example of MCF-7 cells the results of the proliferation tests were confirmed by cell growth analysis (Figure S1). After three days treatment with the combination of TSA and $1\alpha,25(OH)_2D_3$ there were 60% fewer cells than in the vehicle control. At day 5, the combination treatment also inhibited cell growth significantly compared to either $1\alpha,25(OH)_2D_3$ or TSA treatment alone. Both single 5-day-treatments also decreased cell number significantly (75% and 68%) compared to cells treated with vehicle.

To determine, if the lack of proliferation was a result of a block in the cell cycle progression, the three cell lines were treated for two days with ligands and subsequently stained by propidium iodide followed by fluorescence-activated cell sorting (FACS) (Figure 1B). A treatment with TSA alone showed no significant effect on the portion of the cell cycle phase distribution, although we observed a decrease of MCF-7 cells in the S phase and of MDA-MB453 cells in the G_1/G_0 phase. In contrast, $1\alpha,25(OH)_2D_3$ treatment provided a significant increase of MCF-7 and MDA-MB453 cells in the G_1/G_0 phase and a decrease in G_2/M phase. In addition, in MCF-7 cells, a significant decrease of cells in the S phase was also observed after $1\alpha,25(OH)_2D_3$ treatment. Interestingly, in the latter cells, the combined treatment with TSA and $1\alpha,25(OH)_2D_3$ showed an increase of cells in the G_1/G_0 phase and a decrease in the S and G_2/M phase. The effects in MCF-7 cells were significant, not only compared to the vehicle control, but also in reference to the single stimulations with TSA and $1\alpha,25(OH)_2D_3$. In MCF-12A and MDA-MB453 cells the combined treatment resulted only in a significant increase of cells in G_1/G_0 phase. FACS analysis also indicated that the number of apoptotic cells did not change under any stimulation (data not shown) suggesting that in our model cell lines the induction of programmed cell death was not responsible for our results.

Taken together, concerning anti-proliferative effects, via an arrest in the G_1/G_0 phase, the treatment with TSA and $1\alpha,25(OH)_2D_3$, alone and in combination, was most efficient in MCF-7 cells. However, $1\alpha,25(OH)_2D_3$ had also significant anti-proliferative effects in MCF-12A and MDA-MB453 cells.

CDKI gene TSS acetylation and HDAC binding in response to TSA and $1\alpha,25(OH)_2D_3$

The basal mRNA expression levels of the four *CDKI* genes *p18*, *p19*, *p21* and *p27* were monitored by real-time quantitative PCR in relation to the control gene *RPLP0* in MCF-12A, MCF-7 and MDA-MB453 cells (Figure S2A). The three remaining *CDKI* gene family members, *p15, p16* and *p57*, were not expressed to detectable level in all of these cell lines (data not shown) and hence were excluded from further analysis. The genes *p18* and *p21* had the highest basal expression in non-cancerous MCF-12A cells, whereas most *p19* mRNA expression was found in malignant MDA-MB453 cells. The genes *p18* and *p19* were expressed lowest in $p53^+$ MCF-7 cells, whereas the lowest basal mRNA levels of the *p21* gene were detected in $p53^-$ MDA-MB453 cells. In contrast, basal *p27* mRNA expression was not significantly different in the three cell lines.

The acetylation levels of histone H3-K14 and histone H4 on the TSS regions of the genes *p18*, *p19*, *p21* and *p27* in response to 1 h treatment with TSA and $1\alpha,25(OH)_2D_3$ were studied by ChIP assays in all three cell lines (Figure 2A). In parallel, the mRNA induction of the four genes over time in response to these ligands was studied by real-time PCR (time point 3 h in Figure 2B, time points 1, 2, 4 and 6 h in Figure S2B). In general, the

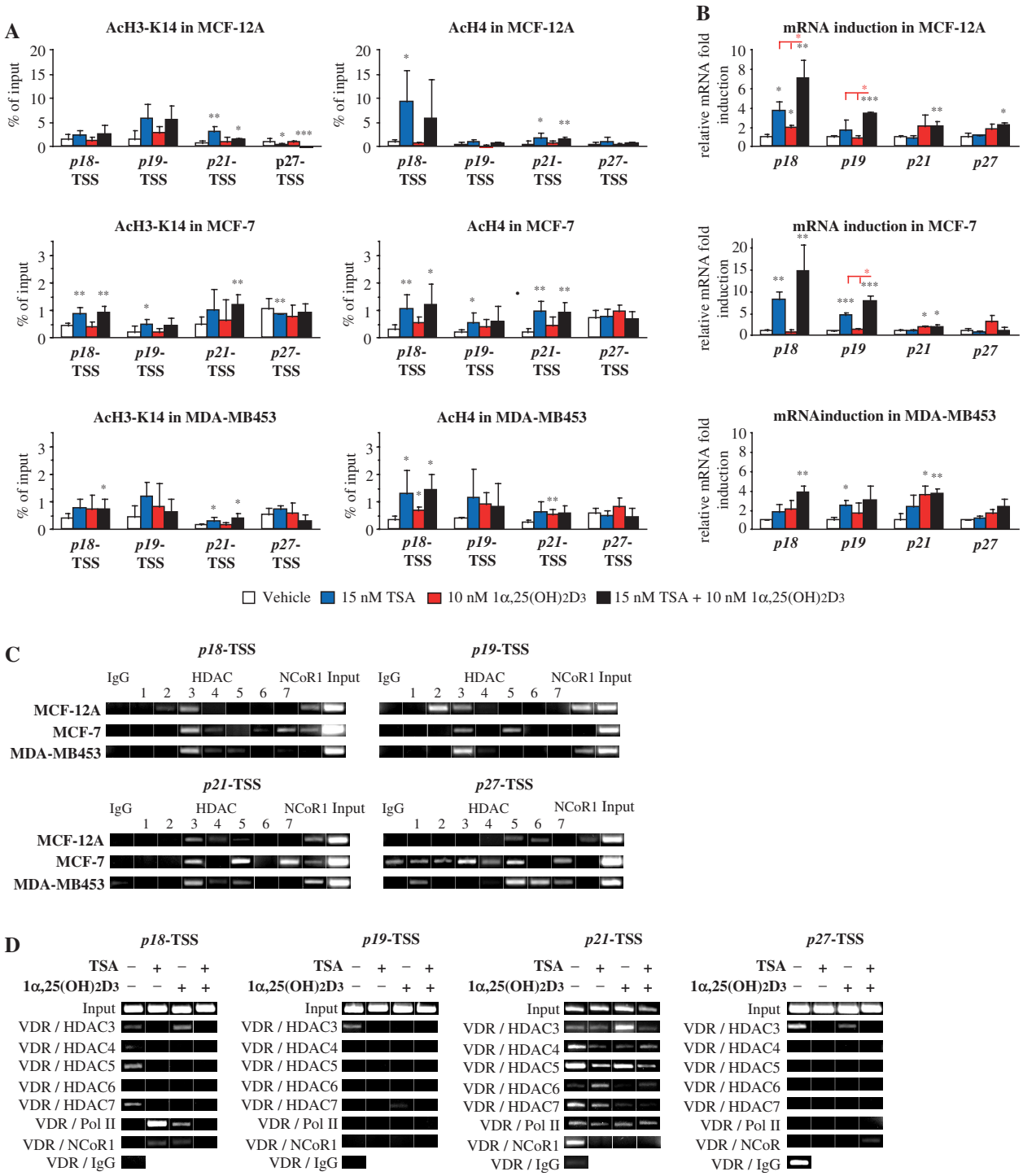

Figure 2. Acetylation and HDAC binding to the TSS regions of *CDKI* genes. (**A**) Chromatin was extracted from MCF-12A, MCF-7 and MDA-MB453 cells that had been treated, alone or in combination, with 15 nM TSA, 10 nM $1\alpha,25(OH)_2D_3$ and EtOH for 1 h and fold inductions were calculated in reference to vehicle control. Acetylation of the TSS of the genes *p18*, *p19*, *p21* and *p27* was analyzed by ChIP assays using anti-AcH3-K14 and anti-AcH4 antibodies, where IgG served as specificity control. The acetylation levels relative to input were determined by quantitative real-time PCR. IgG precipitation was subtracted from quantified acetylation levels. (**B**) After 3 h of ligand treatment the mRNA expression of the four *CDKI* genes relative to the control gene *RPLP0* was determined by real-time quantitative PCR and fold inductions were calculated in reference to vehicle control. Columns indicate the means of at least three independent cell treatments and the bars represent standard deviations. A two-tailed Student's *t*-test was performed to determine the significance of the stimulation in reference to vehicle-treated control ($^{*}P < 0.05$; $^{**}P < 0.01$; $^{***}P < 0.001$). The significance of the co-treatment in comparison to the single stimulations with TSA and $1\alpha,25(OH)_2D_3$ were calculated (red stars). (**C**) The binding of HDACs 1–7 and of NCoR1 to the TSS of the four *CDKI* genes in non-treated cells was determined by ChIP assays using the respective specific antibodies. (**D**) Re-ChIP experiments were performed on the same regions on chromatin that was extracted from MDA-MB453 cells being treated, alone or in combination, with 15 nM TSA, 10 nM $1\alpha,25(OH)_2D_3$ and vehicle (EtOH) for 1 h. Precipitations with IgG served as specificity controls (C and D). Representative agarose gels of the PCR products are shown.

basal acetylations of the *CDKI* gene TSS regions were highest in MCF-12A cells (please note the different scales in Figure 2A). TSA induced the expression of *p18* and *p19* mRNA (11- and 6-fold at 4 h) in MCF-7 cells and of *p18* in MCF-12A cells (Figures 2B and S2B). Comparable effects were observed also concerning the acetylation levels of the *p18*- and *p19*-TSS regions (2-fold for AcH3-K14 and 4-fold for AcH4 in MCF-7 cells). In MCF-12A cells, only the AcH4 level on the *p18*-TSS was significantly induced (10.8-fold). Even in MDA-MB453 cells the AcH4 level on the *p18*-TSS was induced, but this effect was not transmitted to significant mRNA inductions before 6 h of treatment. Expression of *p18* was induced also in MDA-MB453 cells, when higher (100 nM) TSA concentration was used, but with this concentration, all combinatorial effects with $1\alpha,25(OH)_2D_3$ were lost (data not shown). In contrast, *p21* and *p27* mRNA expression was not significantly induced by TSA. Acetylation of the *p27*-TSS was even repressed by TSA, while *p21*-TSS acetylation was induced, but without transmitting this effect into induction of *p21* gene transcription.

In all three cell lines the known $1\alpha,25(OH)_2D_3$ target gene *p21* (17,24) was significantly induced by $1\alpha,25(OH)_2D_3$ (1.6- to 3.6-fold). Additionally, in MCF-12A and MDA-MB453 cells the *p18* gene (1.9- and 1.6-fold), in MCF-7 and MDA-MB453 cells the *p19* gene (1.9- and 1.6-fold) and in MCF-12A and MCF-7 cells the *p27* gene (1.7- and 3.2-fold) responded to $1\alpha,25(OH)_2D_3$ treatment (Figures 2B and S2B). However, in most cases these mRNA inductions were not reflected by changes of the acetylation levels of the respective *CDKI* gene TSS regions (Figure 2A).

In general, the combined treatment with TSA and $1\alpha,25(OH)_2D_3$ resulted in all three cell lines in a higher mRNA expression than either of the substances alone (an exception was the *p27* gene in MCF-7 cells, see Figures 2B and S2B). In a number of cases, such as the *p18* gene in MCF-12A cells, the *p19* gene in MCF-12A and MCF-7 cells, the *p21* gene in MCF-7 and MDA-MB453 cells and the *p27* gene in MDA-MB453 cells, these co-operative effects were also statistically significant.

To elucidate the role of individual HDACs on acetylation changes on the TSS regions of *CDKI* genes, we analyzed by ChIP assays the occupancy of the *CDKI* gene TSS regions for HDAC1 to 7 and NCoR1 (Figure 2C). The most pre-dominant deacetylase enzyme was HDAC3, which was found in all three cell lines associated with the TSS of the genes *p18*, *p19* and *p21*, but did not bind significantly to the *p27*-TSS. NCoR1 was also widely present at the TSS regions of all four *CDKI* genes in all of cell lines. In MDA-MB453 cells, HDAC4 was also bound to the TSS regions of all four genes. HDAC2 bound only to the *p18* and *p19*-TSS regions in MCF-12A cells and HDAC5 to the *p21* and *p27*-TSS regions in all studied cell lines and that of the *p19* gene in MCF-7 cells. In addition, HDAC7 was present on the *p18*, *p21* and *p27*-TSS regions in MCF-7 cells.

For a more detailed analysis of the role of individual HDAC and NCoR1 proteins in the actions of the VDR on the TSS of the four *CDKI* genes, re-ChIP experiments were performed with anti-VDR antibody in the first precipitation and the second precipitation with antibodies against HDAC3, HDAC4, HDAC5, HDAC6, Pol II and NCoR1 in MDA-MD453 cells that were treated, alone and in combination, with TSA and $1\alpha,25(OH)_2D_3$ for 1 h (Figure 2D). In ChIP assays HDACs 3, 4, 5 and 7 were found to bind the CDKI TSSs and to some extent also to VDREs on the *p21* promoter (Figures 2C and 3D, respectively). Therefore, they were selected for reChIP experiments with anti-VDR antibodies. The other HDACs were left out, because they showed no or only low binding on the studied chromatin regions. Under non-stimulated conditions VDR was found on the *p18*-TSS in a complex with HDAC3, HDAC4, HDAC5 and HDAC7. The VDR-HDAC3 complex was resistant against stimulation with $1\alpha,25(OH)_2D_3$ alone, while TSA induced the dissociation of all HDACs. On this TSS TSA and $1\alpha,25(OH)_2D_3$ induced VDR-Pol II and VDR–NCoR1 complexes. On the *p19*-TSS and the *p27*-TSS only VDR–HDAC3 complexes can be detected, which dissociate after stimulation with TSA or $1\alpha,25(OH)_2D_3$. In contrast, on the *p21*-TSS all seven proteins were found in complexes with the VDR. VDR–HDAC3 complexes were enhanced by $1\alpha,25(OH)_2D_3$ alone and VDR–HDAC6 complexes were induced by TSA alone. Both compounds, alone and in combination, reduced VDR–HDAC4 and VDR–NCoR1 complexes on this TSS. The VDR–HDAC5 complex was sensitive to treatments with TSA and the VDR–HDAC7 complex to stimulations with $1\alpha,25(OH)_2D_3$. On the VDR–Pol II complex none of the treatments had a significant effect.

In summary, TSA induced TSS acetylation and mRNA expression of the genes *p18* and *p19*, while $1\alpha,25(OH)_2D_3$-induced *p21* mRNA expression without affecting the overall acetylation status of the *p21*-TSS. The latter divergence also became obvious concerning the combinatorial effects of TSA and $1\alpha,25(OH)_2D_3$. The most striking difference between the *CDKI* gene TSS regions was the lack of HDAC3 and NCoR1 binding to the *p27*-TSS, where also histone acetylation was not induced by TSA. Moreover, on the *p18*- and *p21*-TSS VDR formed complexes with HDACs, Pol II and NCoR1, which were all sensitive to either TSA, $1\alpha,25(OH)_2D_3$ or a combinatorial treatment.

Chromatin looping, TSS acetylation and HDAC binding on VDR-associated regions of the *p21* promoter

To study the effects of TSA and $1\alpha,25(OH)_2D_3$ on the looping to the TSS of those chromatin regions that are known to associate with VDR in the *p21* promoter (17) we used the C3 technique (Figure 3A). MDA-MB453 cells were stimulated for 1 h with the compounds and their chromatin was cross-linked, digested with restriction endonucleases, ligated and analyzed by PCR (Figure 3B). Looping of $1\alpha,25(OH)_2D_3$ responsive regions 1 (*p21*-1, located −2.3 kB from the TSS, primer C), 2 (*p21*-2, −4.5 kB, primer E) and 3 (*p21*-3, −7.1 kB, primer G) were studied using regions located −1.7 kB (primer B), −3.1 kB (primer D) and −6.1 kB (primer F) from the TSS as negative controls. TSA alone was unable to induce any looping of the regions of the *p21* promoter, but

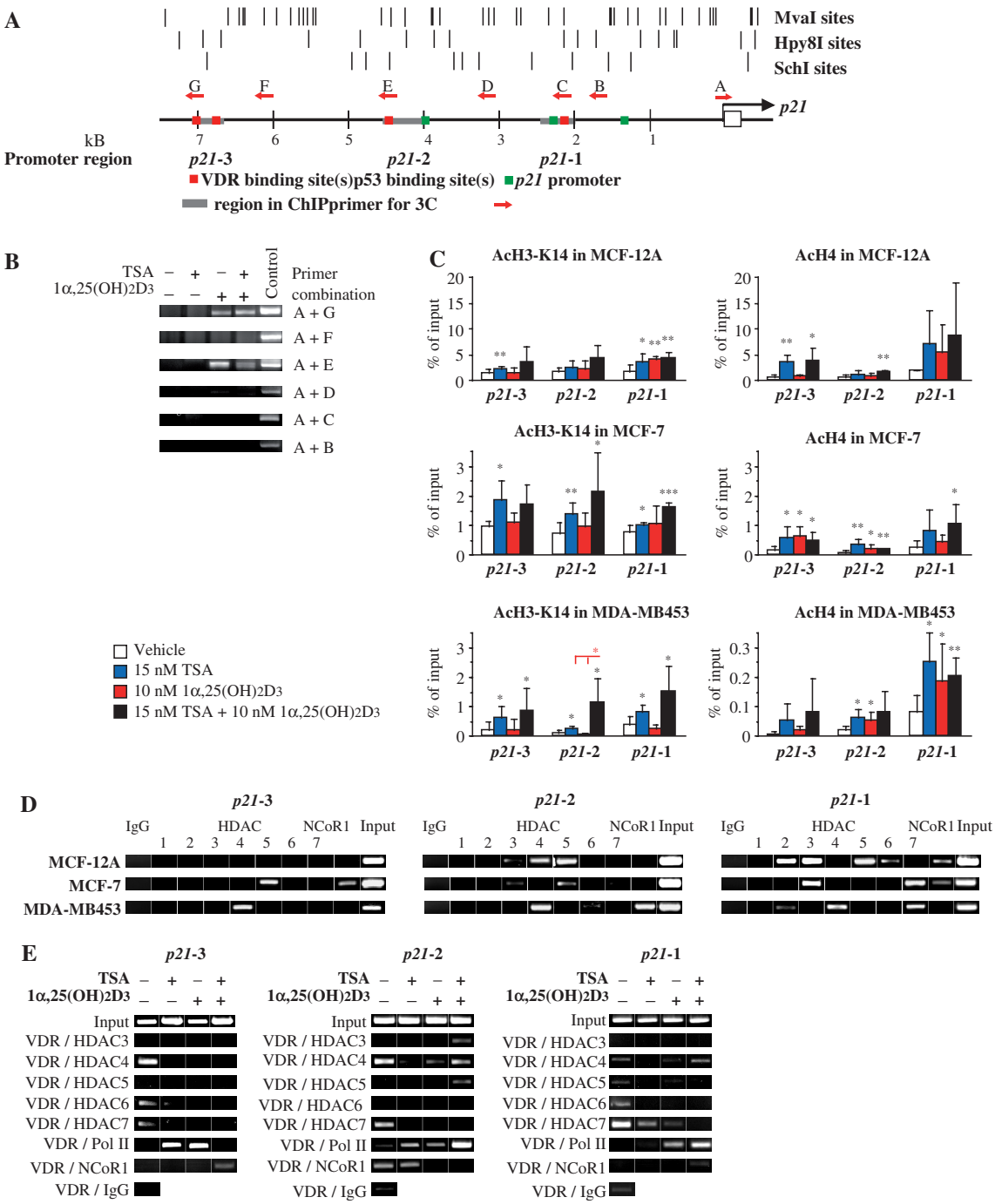

Figure 3. Chromatin looping, acetylation and HDAC binding to VDR-associated regions of the *p21* promoter. (**A**) Schematic overview on the human *p21* promoter indicating VDR and p53 binding sites described previously (17). The location of chromatin regions analyzed by ChIP assays and the restriction enzyme recognition sites and primers used for the C3 assays are shown. (**B**) Chromatin was extracted from MDA-MB453 cells, which had been treated, alone or in combination, with 15 nM TSA, 10 nM $1\alpha,25(OH)_2D_3$ and EtOH for 1 h, cross-linked and digested with the enzymes MvaI, Hpy8I and SchI. After ligation the DNA was extracted and analyzed by PCR with primer A in combination with primers B, C, D, E, F or G. Digestions of subcloned *p21* promoter fragments served as positive controls. Representative agarose gels of the PCR products are shown. (**C**) Chromatin was extracted from MCF-12A, MCF-7 and MDA-MB453 cells that had been treated, alone or in combination, with 15 nM TSA, 10 nM $1\alpha,25(OH)_2D_3$ and EtOH for 1 h. Acetylation of three VDR-associated regions of the *p21* promoter was analyzed by ChIP assays using anti-AcH3-K14 and anti-AcH4 antibodies, where IgG served as specificity control. The acetylation levels relative to input were determined by quantitative real-time PCR. IgG precipitation was subtracted from quantified acetylation levels. Columns indicate the means of at least three independent cell treatments and the bars represent standard deviations. A two-tailed Student's *t*-test was performed to determine the significance of the stimulation in reference to vehicle-treated control ($*P < 0.05$; $**P < 0.01$; $***P < 0.001$). The significance of the co-treatment in comparison to the single stimulations with TSA and $1\alpha,25(OH)_2D_3$ were calculated (red stars). (**D**) The binding of HDACs 1–7 and of NCoR1 to the TSS of the four *CDKI* genes in non-treated cells was determined by ChIP assays using the respective specific antibodies. (**E**) Re-ChIP experiments were performed on the same regions on chromatin that was extracted from MDA-MB453 cells being treated, alone or in combination, with 15 nM TSA, 10 nM $1\alpha,25(OH)_2D_3$ and vehicle (EtOH) for 1 h. Precipitations with IgG served as specificity controls (D and E). Representative agarose gels of the PCR products are shown.

1α,25(OH)$_2$D$_3$ stimulated the association of regions 2 and 3, but not of region 1, with the TSS. The combined treatment with TSA and 1α,25(OH)$_2$D$_3$ did not show any additional effects to what was observed with 1α,25(OH)$_2$D$_3$ alone.

Next we studied in all three cell lines the acetylation levels of the three VDR-associated regions of the *p21* promoter (Figure 3C). Basal acetylation of these chromatin regions was 8.4- and 52-fold higher in non-malignant *p53*$^+$ MCF-12A cells than in metastatic *p53* mutated MDA-MB453 cells for H3-K14 and H4, respectively (please note the different scales in Figure 3C). TSA treatment resulted in all three cell lines and on all three *p21* promoter regions, except for *p21*-2 in MCF-12A cells, a significant increase of H3-K14 acetylation, whilst H4 acetylation changes were insignificant on regions 1 and 2 in MCF-12A cells, on region 1 in MCF-7 cells and on region 3 in MDA-MB453 cells. In contrast to effects on the *CDKI* gene TSS regions (Figure 2A), on VDR-associated regions of the *p21* promoter, 1α,25(OH)$_2$D$_3$ was also able to significantly induce histone acetylation. AcH3-K14 was induced 2.3-fold on region 1 in MCF-12A cells and AcH4 increased 2.3- to 4.2-fold on regions 2 and 3 in MCF-7 cells and on regions 1 and 2 in MDA-MB453 cells. The combined treatment with TSA and 1α,25(OH)$_2$D$_3$ followed the effects of TSA alone with the exception of region 2 in MDA-MB453 cells, where the combination resulted in a significantly higher H3-K14 acetylation than the individual compounds.

The occupancy of the VDR-associated regions of the *p21* promoter with HDACs and NCoR1 (Figure 3D) differed clearly from that of the *CDKI* TSS regions (Figure 2C). HDAC1 was not found at all and HDAC2 only on region 1 in MCF-12A and MDA-MB453 cells. HDAC3 was less dominant than on the TSS regions and only bound to the p53-associated regions 1 and 2 (see Figure 3A and (17)) in *p53*$^+$ cells (i.e. MCF-12A and MCF-7). In MDA-MB453 cells, HDAC4 was found on all three regions and additionally on region 2 in MCF-12A cells. HDAC5 associated with regions 1 and 2 in MCF-12A cells and in MCF-7 cells with regions 2 and 3. HDAC6 was found in MCF-12A cells on region 1 and in MDA-MB453 cells on region 2. HDAC7 associated only with region 1 in MCF-7 and MDA-MB453 cells. Finally, NCoR1 associated in MCF-12A cells with region 1, in MCF-7 cells with regions 1 and 3 and in MDA-MB453 cells with region 2.

Both one-step and two-step ChIP (re-ChIP, performed with MDA-MB 453 cells as described above for TSSs of the CDKI genes) assays the *p21* promoter regions (Figure 3D and 3E, respectively) show that there is a different protein association pattern than the *CDKI* gene TSS regions (Figure 2D). On region 1 of the *p21* promoter, VDR was found in complexes with HDAC4, HDAC5, HDAC6 and HDAC7, and these complexes were sensitive both to TSA and 1α,25(OH)$_2$D$_3$ treatment. Interestingly, 1α,25(OH)$_2$D$_3$ alone stimulated VDR–Pol II complexes on this promoter region and co-stimulation with TSA further enhanced this effect. In the absence of stimulation VDR was detected on region 2 in complexes with HDAC4, HDAC7, Pol II and NCoR1. The VDR–HDAC4 and the VDR–HDAC7 complexes were sensitive to a treatment with both compounds, while the VDR–NCoR1 complex dissociated only after addition of 1α,25(OH)$_2$D$_3$. In contrast, the VDR–Pol II complex was enhanced by both compounds alone and even more by the combination of them. Moreover, the combined ligand treatment also induced the complex formation of VDR with both HDAC3 and HDAC5 on this promoter region. In the basal state, VDR was found on promoter region 3 in complexes with HDAC4, HDAC6 and HDAC7. These complexes dissociated after the addition of either of the compounds. Interestingly, single treatments with TSA and 1α,25(OH)$_2$D$_3$ stimulated the VDR–Pol II association on this promoter region, but not their combination. Instead, this co-treatment resulted in a VDR–NCoR1 complex forming on this region.

Taken together, 1α,25(OH)$_2$D$_3$ but not TSA is able to stimulate looping of VDR-associated distal regions 2 and 3 to the TSS, suggesting that the presence of 1α,25(OH)$_2$D$_3$ is sufficient for the VDR-mediated regulation of the *p21* gene. The VDR-associated regions of the *p21* promoter showed, both in the modulation of their histone acetylation as well in their basal HDAC occupancy, distinct protein association profiles in comparison to the TSS region. Moreover, on the three regions of the *p21* promoter VDR formed complexes with HDACs, Pol II and NCoR1, which were sensitive to either TSA, 1α,25(OH)$_2$D$_3$ or a combinatorial treatment.

Modulation of *CDKI* basal gene activity and ligand responsiveness by siRNA inhibition of *VDR*, *NCoR1* and *HDAC*s

Further indications on the role of VDR, NCoR1 and HDACs 3, 4, 6 and 7 in basal expression, TSA and 1α,25(OH)$_2$D$_3$ inducibility of the four *CDKI* genes were obtained by RNAi experiments (Figures 4, S3 and S4). *NCoR1*, *HDAC3* and *HDAC6* mRNA expression was found to be comparable in the three breast epithelial cell lines, whilst *VDR*, *HDAC4* and *HDAC7* gene expression was highest in MDA-MB453 cells (Figure S3A). Depending on the cell line small inhibitory (si) RNA against *VDR* reduced mRNA expression of its target gene by approximately 70%, *NCoR1* siRNA 50–85%, *HDAC3* siRNA 80–90%, *HDAC4* siRNA 75–90%, *HDAC6* siRNA 70–80% and *HDAC7* siRNA 40–60% (Figure S3B). The downregulation by RNA silencing was also manifested at the protein level of the targeted genes (data not shown). Moreover, the effect of the siRNAs on 1α,25(OH)$_2$D$_3$ signaling was tested by a 3 h stimulation of MCF-7 cells and measuring the modulation of mRNA expression of the potently induced 1α,25(OH)$_2$D$_3$ target gene *24-hydroxylase* (*CYP24A1*, Figure S3C). The approximately 20-fold upregulation of the *CYP24A1* mRNA in MCF-7 cells was completely abolished by *VDR* siRNA knockdown and increased by 50–150% by the siRNA knockdown of the genes *HDAC3*, *HDAC4* and *HDAC7*. In contrast, siRNA knockdown of the *NCoR1* and the *HDAC6* gene both had no significant effect on 1α,25(OH)$_2$D$_3$ signaling. For *NCoR1* silencing

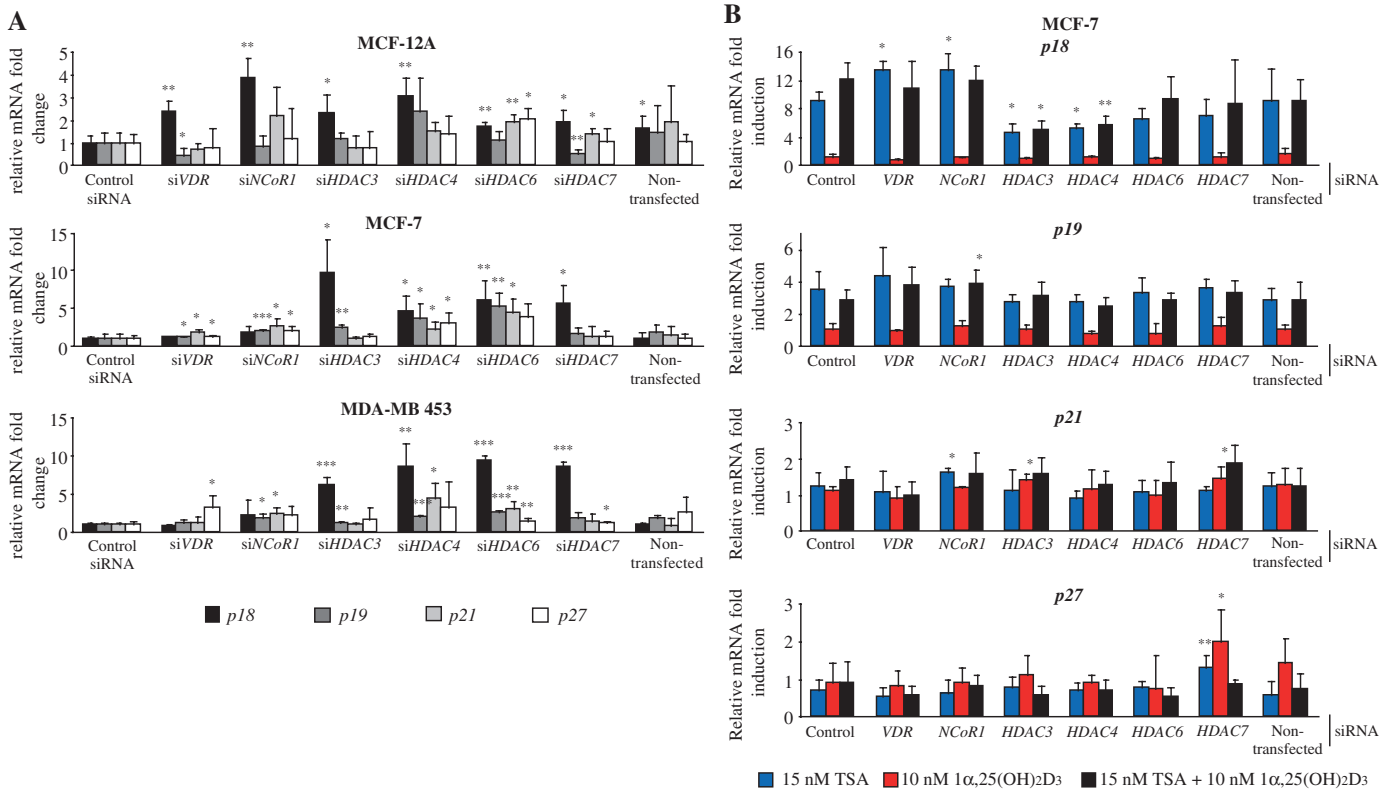

Figure 4. HDACs and NCoR1 have opposite effects on the inducibility of *CDKI* genes. MCF-12A, MCF-7 and MDA-MB453 cells were first transfected for 48 h with siRNA oligonucleotides against VDR, NCoR1, HDAC3, HDAC4, HDAC6 and HDAC7 and then either not treated (**A**) or MCF-7 cells were then stimulated, alone or in combination, with 15 nM TSA, 10 nM $1\alpha,25(OH)_2D_3$ and EtOH for 3 h (**B**, for data of MCF-12A and MDA-MB453 cells see Figure S3). Real-time quantitative PCR was used to determine the mRNA expression of the genes *p18*, *p19*, *p21* and *p27* relative to the control gene *RPLP0* and fold inductions were calculated in reference to control siRNA (A) or vehicle (B). Columns indicate the means of at least three independent cell treatments and the bars represent standard deviations. A two-tailed Student's *t*-test was performed to determine the significance of the stimulation in reference to control siRNA ($^{*}P < 0.05$; $^{**}P < 0.01$; $^{***}P < 0.001$).

no effect was measured, which may be related to low efficacy of siNCoR1 in MCF-7 cells.

The basal expression of the *p18* gene was upregulated by siRNA against all tested *HDACs* in the three cell lines and with higher fold inductions in malignant cell lines (Figure 4A, please note the different scale for MCF-12A cells). In non-malignant MCF-12A cells, *NCoR1* or *VDR* silencing increased *p18* steady state mRNA expression levels. The expression of *p19* mRNA was promoted by siRNA against *NCoR1*, *HDAC3*, *HDAC4* and *HDAC6* in malignant cell lines and by siRNA against *VDR* in MCF-7 cells. On the contrary, in MCF-12A cells, *p19* expression was 2-fold reduced by siRNA against *VDR* and *HDAC7*. Basal expression of the *p21* gene was increased by silencing *NCoR1*, *HDAC4* and *HDAC6* in malignant cell lines and also by silencing *VDR* in MCF-7 cells. In MCF-12A cells, siRNA against *HDAC6* and *HDAC7* uplifted *p21* expression. For *p27* expression, the effects of siRNA were more variable amongst malignant cell lines. In both malignant cell lines, silencing *VDR* increased *p27* expression. Silencing *NCoR1* and *HDAC4* in MCF-7 cells or *HDAC6* and *HDAC7* in MDA-MB453 cells also increased *p27* steady state basal expression levels. In contrast, in MCF-12A cells, only silencing of *HDAC6* promoted *p27* mRNA steady state mRNA expression levels.

The inhibition of the genes *VDR*, *NCoR1* and the four *HDACs* had also an impact on the ligand responsiveness of the four *CDKI* genes (Figures 4B and S4). In MCF-7 cells the response of the *p18* gene to TSA was upregulated by siRNA against *VDR* and *NCoR1* and downregulated by siRNA against *HDAC3* and *HDAC4* (Figure 4B). Moreover, the response of the *p19* gene after stimulation with a combination of TSA and $1\alpha,25(OH)_2D_3$ was significantly increased by *NCoR1* siRNA. The response of the *p21* gene to TSA was promoted by *NCoR1* siRNA and the stimulation by $1\alpha,25(OH)_2D_3$ was enhanced by *HDAC3* and *HDAC7* siRNA. Finally, both the responsiveness of the *p27* gene to TSA and $1\alpha,25(OH)_2D_3$ treatments was increased by *HDAC7* siRNA knockdown. In MCF-12A cells siRNA had only minor effects on ligand responses (Figure S4A). As observed in MCF-7 cells (Figure 4B), also in MDA-MB453 cells the response of the *p18* gene to TSA was upregulated by siRNA against *VDR* and *NCoR1* and downregulated by siRNA against *HDAC3* (Figure S4B). The induction of *p21* by $1\alpha,25(OH)_2D_3$ was abolished with siRNA against either *VDR* or *NCoR1*.

In summary, the most obvious results of these RNAi experiments were that the basal expression of the *p18* gene was repressed in the three cell lines by the four HDACs.

In malignant breast epithelial cells inhibition of VDR and NCoR1 had opposite effects on the stimulation of *p18* gene expression than the block of HDAC3 and HDAC4, whilst in non-malignant cells, siRNA inhibition had hardly any effect on the responsiveness of the *CDKI* genes. Response of the *p21* gene to $1\alpha,25(OH)_2D_3$ was attenuated by *HDAC3* and *HDAC7* in MCF-7 cells, whereas removal of *NCoR1* promoted the basal expression level of the same gene and consequently abolished $1\alpha,25(OH)_2D_3$ induction in MDA-MB453 cells.

DISCUSSION

Anti-proliferative effects both of HDAC inhibitors and $1\alpha,25(OH)_2D_3$ have been linked to changes in the expression of *CDKI* genes (18,25). Based on this, we studied this crossroad of epigenetic and VDR signaling in three mammary cell lines with differential stage of malignancy. For cell treatments we used a low concentration (15 nM) of the HDAC inhibitor TSA, in order to see additional or even co-operative effects with $1\alpha,25(OH)_2D_3$. Although this concentration is sufficient to inhibit HDACs in both malignant cell lines used in this study (26), we observed an anti-proliferative effect of TSA alone only in MCF-7 cells. In contrast, all three cell lines were inhibited in their growth by $1\alpha,25(OH)_2D_3$. The anti-proliferative effect in the two malignant cell lines is due to growth arrest in the G_1/G_0 phase and not based on the induction of apoptosis. Importantly, in MCF-7 cells, we even observed a co-operative anti-proliferative effect between the two compounds, as already previously observed by Banwell and co-workers for the MDA-MB231 malignant mammary cell line (27).

Expression profiling of the four *CDKI* genes *p18*, *p19*, *p21* and *p27*, which are all expressed in the three cell lines, indicated that the TSA-induced growth arrest could be mediated by the induction of INK4 gene family members. In particular, *p18* seems to be the most sensitive and rapidly responding TSA target gene with highest response in MCF-7 cells. This is in accordance with the cell-specific profile of anti-proliferative effects in the tested cell lines. Further support of the idea that the anti-proliferative effect of TSA is mediated by upregulation of *p18* gene expression, is provided by the observation that growth inhibition by TSA was attenuated in mouse embryo fibroblasts lacking *p18* (11). However, in contrast to previous observations (13), in the breast epithelial cells tested here, *p21* does not respond as quickly and to a lesser extent, since we did not observe any mRNA induction earlier than after 6 h of stimulation. Nevertheless, in both malignant mammary cell lines TSA acts co-operatively with $1\alpha,25(OH)_2D_3$ on the induction of the *p21* gene.

General acetylation of histone H4 and acetylation of histone H3 at lysine 14 are associated with active chromatin (28). We observed that the level of histone modifications on the TSS regions of the genes *p18*, *p19* and *p21* is higher in non-malignant MCF-12A cells than in the two malignant mammary cell lines. For *p18* and *p21* this nicely correlates with the basal mRNA expression of these genes, but there must be additional mechanisms that mediate the high basal *p19* expression in MDA-MB453 cells. Interestingly, TSA is able to enhance the level of these histone modifications not only on the *p18*, *p19* and *p21* TSS regions but also on the VDR-associated regions of the *p21* promoter. However, HDAC inhibition did not induce acetylation on the *p27*-TSS as already reported previously (13). This indicates a broad but not completely unspecific effect of TSA on gene activation. The TSA sensitive TSS regions show as a common feature a high basal association with HDAC3 and in most cases also with NCoR1.

In the three tested cell lines there is a consistent, statistically significant upregulation of the *p21* gene by $1\alpha,25(OH)_2D_3$, which supports the idea that this gene is critical for the anti-proliferative effect of $1\alpha,25(OH)_2D_3$. In this study, TSA did not induce *p21* expression contrary to previous reports (29,30). This may be due to differences in the experimental design. For example, the concentration and time of TSA exposure used in our experiments were substantially smaller than those used by others, which were 7–17 h treatment with 25–100 ng/ml (29,30).

Previously, we have identified three VDR-associated regions by ChIP scanning of the *p21* promoter (17) and we used these regions as an example of $1\alpha,25(OH)_2D_3$-responding chromatin. Here we demonstrate that $1\alpha,25(OH)_2D_3$, but not TSA, induces looping of the two more distal regions at positions −4.5 kB and −6.9 kB. However, we could not detect DNA looping of the more proximal region at position −2.3 kB, although on the level of histone acetylation this region responded well to both TSA and $1\alpha,25(OH)_2D_3$ and re-ChIP assays showed $1\alpha,25(OH)_2D_3$-dependent VDR–Pol II complex formation. On all three *p21* promoter regions both TSA and $1\alpha,25(OH)_2D_3$ abolishes the association of VDR with HDAC7 (and to some extent also that with HDAC4 and HDAC6). In MCF-7 cells, HDAC3 and HDAC7 attenuate the response of the *p21* gene to $1\alpha,25(OH)_2D_3$. These cells also have the lowest response of their *p21* gene to $1\alpha,25(OH)_2D_3$ and the highest ratio of HDAC3 to VDR expression.

A previously described model involving the progesterone receptor, proposed that HDAC3 quenches the induction by the ligand and drives the return to the basal state (31) and our data agrees in general with this. When $1\alpha,25(OH)_2D_3$ is combined with TSA or when either *HDAC3* or *HDAC7* gene expression is silenced in $1\alpha,25(OH)_2D_3$-treated cells, the activation of *p21* transcription is prolonged and more mRNA can accumulate. This attenuation of the $1\alpha,25(OH)_2D_3$ response by HDACs is not restricted to the *p21* gene, since the induction of another $1\alpha,25(OH)_2D_3$ induced gene, *CYP24A1*, is also enhanced by silencing either *HDAC3*, *HDAC4* or *HDAC7*. Previously, HDAC3 has been linked to regulation by nuclear receptors via NCoR1/SMRT co-repressor complexes (32), but in a recent study, HDAC3 and HDAC4 were shown to bind nuclear receptors also directly and independently of co-repressor (33). HDAC7 has been found to bind an ERα a target gene in the presence of the ligand (34), analogously to its role in quenching nuclear receptor ligand response in

addition to putative basal repression by un-liganded nuclear receptors. Silencing HDAC expression may also have other, more indirect effects, e.g. via regulation of expression of other co-factors, but this cannot explain the fast combinatorial effects of by TSA and $1\alpha,25(OH)_2D_3$ on the regulation of *CDKI* genes. The regulation of deacetylation activity of HDAC3 and class II HDACs by stimulus-dependent nucleocytoplasmic shuttling (3) enables an additional layer for cell-specific fine-tuning of nuclear receptor response.

RNAi experiments indicated that both NCoR1 and un-liganded VDR appear to be repressors of the basal expression of *CDKI* genes. Elevated NCoR1 levels have been linked with suppressed target gene response to $1\alpha,25(OH)_2D_3$ both in mammary cell lines and in primary breast cancer tumors (35), but paradoxically, we found that silencing the *NCoR1* gene transcriptionally, abolished the induction of the *p21* gene by $1\alpha,25(OH)_2D_3$. Our results suggest that $1\alpha,25(OH)_2D_3$ is unable to induce the *p21* gene in the absence of NCoR1, since release from repression by VDR–NCoR1 complexes (either by ligand application or by inhibiting *NCoR1* expression) raises the basal expression level to the same extent. Therefore, one can assume that the optimal level of NCoR1 expression is essential to the ligand responsiveness.

As expected, silencing HDACs decreased mRNA induction by TSA. However, it is still surprising that silencing of either HDAC3 or HDAC4 alone already reduced the TSA induction of the *p18* gene by 50%. This suggests that both HDACs have a central role in mediating the effects of HDAC inhibitors on the regulation of the *p18* gene. The strong overlap between genes inducible with TSA (either 15 or 100 nM) or by the inhibition of HDAC3 in the three tested cell lines further supports the idea that HDAC3 is the main target of TSA in regulating *CDKI* genes. Since HDAC3 is ubiquitously expressed, knockdown of HDAC3 should have broad and tissue-unspecific consequences to the response to $1\alpha,25(OH)_2D_3$ and TSA. On the other hand, silencing either HDAC4 or HDAC6 induced the expression of *CDKI* genes more broadly, independently of their responsiveness to TSA. Additionally, according to our ChIP experiments, HDAC4 and HDAC6 were not associated with the target gene's TSS regions to an extent that could explain induction upon their removal. This suggests more complex processes than a swift increase in histone acetylation. For example, the role of HDAC6 in proteasomal degradation of misfolded proteins may contribute to upregulation of CDKI genes upon knockdown of HDAC6 (7).

In conclusion, our studies suggest an overlap of the anti-proliferative effects of the HDAC inhibitor TSA and the nuclear receptor ligand $1\alpha,25(OH)_2D_3$ in mammary cell lines. Transcriptional induction by both TSA and $1\alpha,25(OH)_2D_3$ is strongly linked to HDAC and NCoR1 but with opposite consequences, they act through different pathways. HDACs, especially HDAC3, are rate-limiting factors in the termination of ligand-induced transcription, where NCoR1 is not essential, whereas NCoR1 is rate limiting in transcriptional repression afforded by un-liganded VDR, while active HDACs are not essential. The attenuation of the $1\alpha,25(OH)_2D_3$ response by HDACs or of the TSA response by NCoR1 can be overcome by combing these substances to achieve maximal induction of anti-proliferative target genes.

SUPPLEMENTARY DATA

Supplementary Data are available at NAR Online.

ACKNOWLEDGEMENTS

We would like to thank Dr Lise Binderup for $1\alpha,25(OH)_2D_3$, Dr Thomas W. Dunlop for carefully reading the manuscript and Maija Hiltunen for skilled technical assistance. Grants from the Academy of Finland, the Finnish Cancer Organisation and the Juselius Foundation supported this research. Funding to pay the Open Access publication charges for this article was provided by the University of Luxembourg.

Conflict of interest statement. None declared.

REFERENCES

1. Minucci,S. and Pelicci,P.G. (2006) Histone deacetylase inhibitors and the promise of epigenetic (and more) treatments for cancer. *Nat. Rev. Cancer*, **6**, 38–51.
2. Marks,P.A., Miller,T. and Richon,V.M. (2003) Histone deacetylases. *Curr. Opin. Pharmacol.*, **3**, 344–351.
3. Gallinari,P., Di Marco,S., Jones,P., Pallaoro,M. and Steinkühler,C. (2007) HDACs, histone deacetylation and gene transcription: from molecular biology to cancer therapeutics. *Cell. Res.*, **17**, 195–211.
4. Codina,A., Love,J.D., Li,Y., Lazar,M.A., Neuhaus,D. and Schwabe,J.W. (2005) Structural insights into the interaction and activation of histone deacetylase 3 by nuclear receptor corepressors. *Proc. Natl Acad. Sci. USA*, **102**, 6009–6014.
5. Verdin,E., Dequiedt,F. and Kasler,H.G. (2003) Class II histone deacetylases: versatile regulators. *Trends Genet.*, **19**, 286–293.
6. Dequiedt,F., Kasler,H., Fischle,W., Kiermer,V., Weinstein,M., Herndier,B.G. and Verdin,E. (2003) HDAC7, a thymus-specific class II histone deacetylase, regulates Nur77 transcription and TCR-mediated apoptosis. *Immunity*, **18**, 687–698.
7. Kawaguchi,Y., Kovacs,J.J., McLaurin,A., Vance,J.M., Ito,A. and Yao,T.P. (2003) The deacetylase HDAC6 regulates aggresome formation and cell viability in response to misfolded protein stress. *Cell*, **115**, 727–738.
8. Monneret,C. (2005) Histone deacetylase inhibitors. *Eur. J. Med. Chem.*, **40**, 1–13.
9. Li,H. and Wu,X. (2004) Histone deacetylase inhibitor, Trichostatin A, activates $p21^{WAF1/CIP1}$ expression through downregulation of c-myc and release of the repression of c-myc from the promoter in human cervical cancer cells. *Biochem. Biophys. Res. Commun.*, **324**, 860–867.
10. Gui,C.Y., Ngo,L., Xu,W.S., Richon,V.M. and Marks,P.A. (2004) Histone deacetylase (HDAC) inhibitor activation of $p21^{WAF1}$ involves changes in promoter-associated proteins, including HDAC1. *Proc. Natl Acad. Sci. USA*, **101**, 1241–1246.
11. Yokota,T., Matsuzaki,Y., Miyazawa,K., Zindy,F., Roussel,M.F. and Sakai,T. (2004) Histone deacetylase inhibitors activate INK4d gene through Sp1 site in its promoter. *Oncogene*, **23**, 5340–5349.
12. Yokota,T., Matsuzaki,Y. and Sakai,T. (2004) Trichostatin A activates $p18^{INK4c}$ gene: differential activation and cooperation with p19INK4d gene. *FEBS Lett.*, **574**, 171–175.
13. Richon,V.M., Sandhoff,T.W., Rifkind,R.A. and Marks,P.A. (2000) Histone deacetylase inhibitor selectively induces $p21^{WAF1}$ expression

and gene-associated histone acetylation. *Proc. Natl Acad. Sci. USA*, **97**, 10014–10019.
14. Malumbres,M. and Barbacid,M. (2007) Cell cycle kinases in cancer. *Curr. Opin. Genet. Dev.*, **17**, 60–65.
15. Guan,K.L., Jenkins,C.W., Li,Y., Nichols,M.A., Wu,X., O'Keefe,C.L., Matera,A.G. and Xiong,Y. (1994) Growth suppression by p18, a $p16^{INK4/MTS1}$- and $p14^{INK4B/MTS2}$-related CDK6 inhibitor, correlates with wild-type pRb function. *Genes. Dev.*, **8**, 2939–2952.
16. Hirai,H., Roussel,M.F., Kato,J.-Y., Ashmun,R.A. and Sherr,C.J. (1995) Novel INK4 proteins, p18 and p19, are specific inhibitors of the cyclin D-dependent kinases CDK4 and CDK6. *Mol. Cell. Biol.*, **15**, 2672–2681.
17. Saramäki,A., Banwell,C.M., Campbell,M.J. and Carlberg,C. (2006) Regulation of the human $p21^{(waf1/cip1)}$ gene promoter via multiple binding sites for p53 and the vitamin D_3 receptor. *Nucleic Acids Res.*, **34**, 543–554.
18. Liu,M., Lee,M.-H., Cohen,M., Bommakanti,M. and Freedman,L.P. (1996) Transcriptional activation of the Cdk inhibitor p21 by vitamin D_3 leads to the induced differentiation of the myelomonocytic cell line U937. *Genes. Dev.*, **10**, 142–153.
19. Kaldis,P. (2007) Another piece of the $p27^{Kip1}$ puzzle. *Cell*, **128**, 241–244.
20. Polly,P., Herdick,M., Moehren,U., Baniahmad,A., Heinzel,T. and Carlberg,C. (2000) VDR-Alien: a novel, DNA-selective vitamin D_3 receptor-corepressor partnership. *FASEB J.*, **14**, 1455–1463.
21. Sutton,A.L. and MacDonald,P.N. (2003) Vitamin D: more than a "bone-a-fide" hormone. *Mol. Endocrinol.*, **17**, 777–791.
22. Mørk Hansen,C., Binderup,L., Hamberg,K.J. and Carlberg,C. (2001) Vitamin D and cancer: effects of $1,25(OH)_2D_3$ and its analogs on growth control and tumorigenesis. *Front Biosci.*, **6**, D820–D848.
23. Rachez,C., Lemon,B.D., Suldan,Z., Bromleigh,V., Gamble,M., Näär,A.M., Erdjument-Bromage,H., Tempst,P. and Freedman,L.P. (1999) Ligand-dependent transcription activation by nuclear receptors requires the DRIP complex. *Nature*, **398**, 824–828.
24. Jiang,H., Lin,J., Su,Z.-z., Collart,F.R., Huberman,E. and Fisher,P.B. (1994) Induction of differentiation in human promyelotic HL-60 leukemia cells activates p21, WAF1/CIP1, expression in the absence of p53. *Oncogene*, **9**, 3397–3406.
25. Warrener,R., Beamish,H., Burgess,A., Waterhouse,N.J., Giles,N., Fairlie,D. and Gabrielli,B. (2003) Tumor cell-selective cytotoxicity by targeting cell cycle checkpoints. *FASEB J.*, **17**, 1550–1552.
26. Vigushin,D.M., Ali,S., Pace,P.E., Mirsaidi,N., Ito,K., Adcock,I. and Coombes,R.C. (2001) Trichostatin A is a histone deacetylase inhibitor with potent antitumor activity against breast cancer in vivo. *Clin. Cancer Res.*, **7**, 971–976.
27. Banwell,C.M., O'Neill,L.P., Uskokovic,M.R. and Campbell,M.J. (2004) Targeting $1\alpha,25$-dihydroxyvitamin D_3 antiproliferative insensitivity in breast cancer cells by co-treatment with histone deacetylation inhibitors. *J. Steroid Biochem. Mol. Biol.* 89–90, 245–249.
28. Strahl,B.D. and Allis,C.D. (2000) The language of covalent histone modifications. *Nature*, **403**, 41–45.
29. Margueron,R., Licznar,A., Lazennec,G., Vignon,F. and Cavailles,V. (2003) Oestrogen receptor alpha increases $p21^{(WAF1/CIP1)}$ gene expression and the antiproliferative activity of histone deacetylase inhibitors in human breast cancer cells. *J. Endocrinol.*, **179**, 41–53.
30. Xiao,H., Hasegawa,T. and Isobe,K. (1999) Both Sp1 and Sp3 are responsible for $p21^{waf1}$ promoter activity induced by histone deacetylase inhibitor in NIH3T3 cells. *J. Cell. Biochem.*, **73**, 291–302.
31. Aoyagi,S. and Archer,T.K. (2007) Dynamic histone acetylation/deacetylation with progesterone receptor-mediated transcription. *Mol. Endocrinol.*, **21**, 843–856.
32. Ishizuka,T. and Lazar,M.A. (2003) The N-CoR/histone deacetylase 3 complex is required for repression by thyroid hormone receptor. *Mol. Cell. Biol.*, **23**, 5122–5131.
33. Franco,P.J., Li,G. and Wei,L.N. (2003) Interaction of nuclear receptor zinc finger DNA binding domains with histone deacetylase. *Mol. Cell. Endocrinol.*, **206**, 1–12.
34. Metivier,R., Penot,G., Hubner,M.R., Reid,G., Brand,H., Kos,M. and Gannon,F. (2003) Estrogen receptor a directs ordered, cyclical, and combinatorial recruitment of cofactors on a natural target promoter. *Cell*, **115**, 751–763.
35. Banwell,C.M., MacCartney,D.P., Guy,M., Miles,A.E., Uskokovic,M.R., Mansi,J., Stewart,P.M., O'Neill,L.P., Turner,B.M. *et al.* (2006) Altered nuclear receptor corepressor expression attenuates vitamin D receptor signaling in breast cancer cells. *Clin. Cancer Res.*, **12**, 2004–2013.